THEORETICAL AND APPLIED MECHANICS
Volume 45 (2018) Issue 2, 189–203 DOI: https://doi.org/10.2298/TAM180424008P

ASYMPTOTIC SOLUTION FOR THE DARCY–BRINKMAN–BOUSSINESQ FLOW IN A PIPE WITH HELICOIDAL SHAPE

Igor Pažanin

Dedicated to the memory of my mother Milica.
I love you and miss you, Mama.

Abstract. We study the fluid flow and heat transfer in a helical pipe filled with a sparsely packed porous medium. Motivated by the engineering applications, pipe's thickness and the distance between two coils of the helix have the same small order of magnitude, whereas the fluid inside the pipe is assumed to be cooled (or heated) by the exterior medium. After writing the dimensionless Darcy–Brinkman–Boussinesq system in curvilinear coordinates, we employ the multi-scale expansion technique to formally derive the effective model valid for small Brinkman–Darcy number. The obtained asymptotic solution is given in the explicit form which is important with regards to numerical simulations. Comparison with our previous results on the straight-pipe flow is also provided.

1. Introduction

Due to its importance from the practical point of view, curved-pipe flows have been the subject of numerous investigations for many years. The pioneer researcher is Dean [1] who studied the fluid flow through a curved circular pipe by the perturbation method, back in 1927. Among various geometries of the curved pipe, helically coiled pipe seems to attract the most attention due to its compactness–increased surface of the pipe within the same volume. In view of that, one can find many papers dealing with the helical-pipe flow, both theoretically and experimentally. Here we mention only those that influenced our work. The isothermal fluid flow through a helical pipe with no porous structure inside has been investigated in [2–11]. The main idea in the analytical papers of those was to employ the curvilinear coordinates attached to the Frenet basis of the helix and to write the governing equations in such basis. A comprehensive overview of the work done on flow and heat transfer characteristics in curved tubes has been provided in [12] and we refer the reader to the large list of references therein. Asymptotic behavior

2010 *Mathematics Subject Classification:* 35B40; 35Q35; 76S05.
Key words and phrases: helical pipe, Darcy-Brinkman-Boussinesq system, Newton cooling condition, curvilinear coordinates, asymptotic approximation.

of the heat flow through a pipe with helicoidal shape has been investigated in [13] by the author of the present paper (see also [14] for the general curved pipe).

Our goal here is to address a non-isothermal fluid flow through a helical pipe filled with sparsely packed porous medium. We assume that the pipe's thickness and the helix step (the distance between two coils of the helix) have the same small order $\mathcal{O}(\varepsilon)$, $0 < \varepsilon \ll 1$, while the diameter of the helix is of order $\mathcal{O}(1)$ (see Figure 1). Such assumptions cover a large variety of realistic coiled pipes appearing naturally in many applications, in particular those related to geophysical systems. To keep the considered problem in line with the applications, the pipe is supposed to be plunged in an exterior bath maintained at a temperature different than the fluid temperature inside the pipe. To describe the porous medium flow inside the pipe, we employ a fully coupled nonlinear Darcy–Brinkman–Boussinesq (DBB) model. DBB model represents the thermodynamic closure of the Brinkman-extended Darcy flow model which allows physically relevant no-slip condition to be imposed on an impermeable boundary (see e.g. [15, 16]). Boussinesq approximation is based on the assumption that the variations of the fluid density can be ignored everywhere except in the vital buoyancy term involving the thermal expansion coefficient. We refer the reader to [17–19].

The survey of the existing literature on the subject indicates that the analytical results have been reported mostly for straight-pipe flows, see e.g., [20–22]. In the case of the porous medium occupying the helical pipe, it seems that only one result has been published, namely by Nield and Kuznetsov [23] (see also [24] for numerical simulations). In [23], the authors employ the simple Darcy model (which cannot handle the no-slip boundary condition imposed on an impermeable wall) and present the perturbation analysis in the case when the curvature κ and the torsion τ of the pipe's central curve are both $\mathcal{O}(\varepsilon)$. No heat exchange between the fluid inside the pipe and the surrounding medium is taken into account. In the present paper, we aim to study the more general Darcy–Brinkman–Boussinesq flow and, in addition, we allow the heat exchange through the pipe's lateral boundary by prescribing the Robin boundary condition. Moreover, the helical pipe under consideration is such that $\kappa = \mathcal{O}(1)$ and $\tau = \mathcal{O}(\varepsilon)$ making the problem more challenging from the point of view of asymptotic analysis. Indeed, in this setting, Frenet basis depends on small parameter ε in an inconvenient way (it follows the pipe's coils and thus oscillates with period ε) and certain precautions in that direction should be undertaken.

The paper is organized as follows. In Section 2, we describe the domain's geometry and introduce the flow equations endowed with the boundary conditions. We choose to work in non-dimensional setting because we aim to compare the characteristic numbers of the problem with small parameter ε. In Section 3, we write the governing problem in curvilinear coordinates using the modified basis appropriate for further asymptotic analysis. In Section 4, we use the two-scale expansion technique (with respect to ε) to derive the asymptotic approximation for the unknown velocity, pressure and temperature of the fluid. It should be emphasized that we manage to explicitly compute the zero-order approximation and also the higher-order correctors and that represents our main contribution.

By doing that, we can straightforwardly compare the obtained results with the one obtained for straight-pipe flow in Beneš and Pažanin [22] (see Section 5) and detect the effects of pipe's distortion on the macroscopic flow. In Section 5 we also comment on the possible outcomes of the theoretical error analysis. To conclude, we firmly believe that provided higher-order asymptotic model can upgrade the numerical simulations of helical pipe flows and improve the known engineering practice related to thermoconductive porous medium flow.

2. Description of the problem

2.1. The geometry of the domain. Let $(\mathbf{e}_1, \mathbf{e}_2, \mathbf{e}_3)$ be the orthonormal basis as depicted in Figure 1. We assume that the pipe's central curve follows a helix given by a parametrization:

$$\mathbf{r}_\varepsilon(x_1) = x_1\mathbf{e}_1 + a\cos\frac{x_1}{\varepsilon}\,\mathbf{e}_2 + a\sin\frac{x_1}{\varepsilon}\,\mathbf{e}_3, \quad x_1 \in [0,1], \tag{2.1}$$

where $a > 0$ is a (non-dimensional) given parameter.

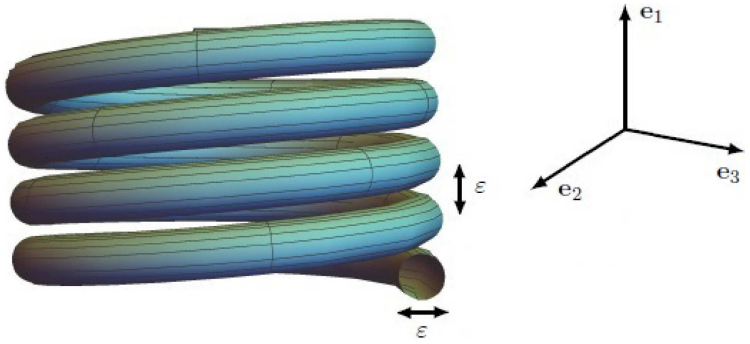

FIGURE 1. Helical pipe.

The corresponding Frenet basis attached to a helix is computed as follows:

$$\mathbf{t}_\varepsilon(x_1) = \frac{1}{\left|\frac{d\mathbf{r}_\varepsilon}{dx_1}\right|}\frac{d\mathbf{r}_\varepsilon}{dx_1} = \frac{1}{\sqrt{a^2+\varepsilon^2}}\Big(\varepsilon\,\mathbf{e}_1 - a\sin\frac{x_1}{\varepsilon}\,\mathbf{e}_2 + a\cos\frac{x_1}{\varepsilon}\,\mathbf{e}_3\Big), \tag{2.2}$$

$$\mathbf{n}_\varepsilon(x_1) = \frac{1}{\left|\frac{d\mathbf{t}_\varepsilon}{dx_1}\right|}\frac{d\mathbf{t}_\varepsilon}{dx_1} = -\cos\frac{x_1}{\varepsilon}\,\mathbf{e}_2 - \sin\frac{x_1}{\varepsilon}\,\mathbf{e}_3, \tag{2.3}$$

$$\mathbf{b}_\varepsilon(x_1) = \mathbf{t}_\varepsilon \times \mathbf{n}_\varepsilon = \frac{1}{\sqrt{a^2+\varepsilon^2}}\Big(a\,\mathbf{e}_1 + \varepsilon\sin\frac{x_1}{\varepsilon}\,\mathbf{e}_2 - \varepsilon\cos\frac{x_1}{\varepsilon}\,\mathbf{e}_3\Big). \tag{2.4}$$

We first introduce a straight pipe with circular cross section

$$S_\varepsilon = \{x = (x_1, x_2, x_3) \in \mathbf{R}^3 : x_1 \in (0,1),\ x' = (x_2, x_3) \in \varepsilon B\} \tag{2.5}$$

with $\varepsilon > 0$ being non-dimensional small parameter and $B = B(0,1) \subset \mathbf{R}^2$ a unit circle. Employing the mapping

$$\mathbf{\Phi}_\varepsilon \colon S_\varepsilon \to \mathbf{R}^3, \quad \mathbf{\Phi}_\varepsilon(x) = \mathbf{r}_\varepsilon(x_1) + x_2\mathbf{n}_\varepsilon(x_1) + x_3\mathbf{b}_\varepsilon(x_1), \tag{2.6}$$

we define

$$\Omega_\varepsilon = \mathbf{\Phi}_\varepsilon(S_\varepsilon). \tag{2.7}$$

Ω_ε represents our three-dimensional domain (see Figure 1) describing a helical pipe whose thickness and the distance between two coils are of same small order of magnitude, namely $\mathcal{O}(\varepsilon)$. The pipe's lateral boundary and its ends are denoted by

$$\Gamma_\varepsilon = \mathbf{\Phi}_\varepsilon((0,1)\times\varepsilon\partial B), \quad \Sigma_i^\varepsilon = \mathbf{\Phi}_\varepsilon(\{i\}\times\varepsilon B), \qquad i = 0,1. \tag{2.8}$$

2.2. The equations and boundary conditions. The helical pipe Ω_ε is filled by a fluid-saturated sparsely packed porous medium. In view of that, the flow and heat transfer is governed by the Darcy–Brinkman–Boussinesq model written in the non-dimensional form:

$$\mathbf{u}_\varepsilon - \widetilde{Da}_\varepsilon\Delta\mathbf{u}_\varepsilon + \nabla p_\varepsilon = Ra_D T_\varepsilon\,\mathbf{e}_1 \qquad \text{in} \quad \Omega_\varepsilon, \tag{2.9}$$

$$\operatorname{div}\mathbf{u}_\varepsilon = 0 \qquad \text{in} \quad \Omega_\varepsilon, \tag{2.10}$$

$$-\Delta T_\varepsilon + \mathbf{u}_\varepsilon\cdot\nabla T_\varepsilon = 0 \qquad \text{in} \quad \Omega_\varepsilon. \tag{2.11}$$

The above system is endowed with the following boundary conditions:

$$\mathbf{u}_\varepsilon = 0, \quad \frac{\partial T_\varepsilon}{\partial\nu_\varepsilon} = Nu_\varepsilon(\mathcal{G} - T_\varepsilon) \qquad \text{on} \quad \Gamma_\varepsilon, \tag{2.12}$$

$$\mathbf{u}_\varepsilon\times\mathbf{t}_\varepsilon = 0, \quad p_\varepsilon = q_i, \quad T_\varepsilon = T_i \qquad \text{on} \quad \Sigma_i^\varepsilon,\ i = 0,1. \tag{2.13}$$

Following real-life applications, we take into account the possible heat exchange between surrounding medium and the fluid inside the pipe so we impose Newton's cooling law $(2.12)_2$. Here, ν_ε denotes the exterior unit normal on the lateral boundary, whereas $\mathcal{G}$ is a given bounded function of the form $\mathcal{G}(z) = G(x_1)$, $z = \mathbf{\Phi}_\varepsilon(x)$ standing for the dimensionless temperature of the surrounding medium. To close up the boundary-value problem, we prescribe the constant pressures q_i at pipe's ends, as well as the constant boundary temperatures T_i. The characteristic numbers of the problem are defined by (see [17]):

$$\widetilde{Da}_\varepsilon = \frac{\nu_{\text{eff}}K}{\nu\ell^2} \quad \text{(Brinkman–Darcy number)}, \tag{2.14}$$

$$Ra_D = \frac{g\beta\delta_T K\ell}{\nu\kappa} \quad \text{(Rayleigh–Darcy number)}, \tag{2.15}$$

$$Nu_\varepsilon = \frac{\beta\ell}{\kappa\delta_T} \quad \text{(Nusselt number)}, \tag{2.16}$$

Here ν is the (kinematic) viscosity of the fluid, ν_{eff} is the effective (kinematic) viscosity of the fluid in the porous medium, K stands for the permeability of the porous medium, g denotes the gravitational acceleration constant, β is the coefficient of the thermal expansion, δ_T is the (dimensional) temperature difference between the pipe's ends, while κ represents the thermal conductivity.

In the sequel, we set $Ra_D = \mathcal{O}(1)$. On the other hand, we take $\widetilde{Da}_\varepsilon = \varepsilon$ since in most applications the classical Darcy number $Da = \frac{K}{\ell^2}$ is of small order of magnitude (see [17]). Following our previous results on the pipe flow, we expect to deduce different effective models depending on the order of magnitude of Nu^ε

with respect to ε. We shall detect the most interesting one (in which all the physical relevant effects are balanced) and perform the asymptotic analysis in this critical case.

3. The problem in curvilinear coordinates

In this section, we write the governing problem in the curvilinear coordinates (x_i). The approach is based on the introduction of a pair of covariant and contravariant basis for the mapping $\mathbf{\Phi}_\varepsilon$. The vectors of covariant basis, defined by $\mathbf{a}_i(x) = \frac{\partial \mathbf{\Phi}_\varepsilon}{\partial x_i}(x)$, read

$$\mathbf{a}_1 = \frac{x_2 - a}{\varepsilon}\mathbf{e}_\varepsilon - \frac{x_3}{\sqrt{a^2+\varepsilon^2}}\mathbf{n}_\varepsilon + \mathbf{e}_1, \tag{3.1}$$

$$\mathbf{a}_2 = \mathbf{n}_\varepsilon, \quad \mathbf{a}_3 = \frac{\varepsilon}{\sqrt{a^2+\varepsilon^2}}\mathbf{e}_\varepsilon + \frac{a}{\sqrt{a^2+\varepsilon^2}}\mathbf{e}_1, \tag{3.2}$$

where $\mathbf{e}_\varepsilon(x_1) = \sin\frac{x_1}{\varepsilon}\mathbf{e}_2 - \cos\frac{x_1}{\varepsilon}\mathbf{e}_3$. The contravariant basis consists of the vectors $\mathbf{a}^i \cdot \mathbf{a}_j = \delta_{ij}$, leading to

$$\mathbf{a}^1 = -\frac{a\varepsilon}{a^2 - a\,x_2 + \varepsilon^2}\mathbf{e}_\varepsilon + \frac{\varepsilon^2}{a^2 - a\,x_2 + \varepsilon^2}\mathbf{e}_1, \tag{3.3}$$

$$\mathbf{a}^2 = -\frac{a\varepsilon x_3}{\sqrt{a^2+\varepsilon^2}(a^2 - a\,x_2 + \varepsilon^2)}\mathbf{e}_\varepsilon + \mathbf{n}_\varepsilon + \frac{\varepsilon^2 x_3}{\sqrt{a^2+\varepsilon^2}(a^2 - a\,x_2 + \varepsilon^2)}\mathbf{e}_1, \tag{3.4}$$

$$\mathbf{a}^3 = \frac{\varepsilon\sqrt{a^2+\varepsilon^2}}{a^2 - a\,x_2 + \varepsilon^2}\mathbf{e}_\varepsilon + \frac{(a-x_2)\sqrt{a^2+\varepsilon^2}}{a^2 - a\,x_2 + \varepsilon^2}\mathbf{e}_1. \tag{3.5}$$

The following has been observed in [9, 10]: the vector $\mathbf{a}_1$ contains negative power of ε so writing the equations in the pair of basis $(\mathbf{a}^i, \mathbf{a}_i)$ would not be convenient for further asymptotic analysis. Hence, we go back to Frenet basis $(\mathbf{t}_\varepsilon, \mathbf{n}_\varepsilon, \mathbf{b}_\varepsilon)$ and notice that $\mathbf{b}_\varepsilon \to \mathbf{e}_1$ uniformly in x_1, whereas $|\mathbf{t}_\varepsilon + \mathbf{e}_\varepsilon| \to 0$ uniformly in x_1. For that reason, the ideal choice for further analysis would be the basis $(\mathbf{e}_\varepsilon, \mathbf{n}_\varepsilon, \mathbf{e}_1)$.

In view of that, let us introduce

$$\mathbf{U}_\varepsilon = \mathbf{u}_\varepsilon \circ \mathbf{\Phi}_\varepsilon = V_\varepsilon^1\mathbf{e}_\varepsilon + V_\varepsilon^2\mathbf{n}_\varepsilon + V_\varepsilon^3\mathbf{e}_1, \tag{3.6}$$

$$P_\varepsilon = p_\varepsilon \circ \mathbf{\Phi}_\varepsilon, \quad \theta_\varepsilon = T_\varepsilon \circ \mathbf{\Phi}_\varepsilon. \tag{3.7}$$

Now we have to write each differential operator from (2.9)–(2.11) in curvilinear coordinates. Essentially, this has already been done in [10, 13], so we omit the computation details. Taking into account that $\widetilde{Da}_\varepsilon = \varepsilon$ and neglecting the terms with higher powers of ε, the Darcy–Brinkman–Boussinesq system takes the following form:

$$-\varepsilon\Big(\frac{\partial^2 V_\varepsilon^1}{\partial x_2^2} + \frac{\partial^2 V_\varepsilon^1}{\partial x_3^2} + \frac{1}{a}\frac{\partial V_\varepsilon^1}{\partial x_2} - \frac{1}{a^2}V_\varepsilon^1\Big) + V_\varepsilon^1 - \frac{\varepsilon}{a}\frac{\partial P_\varepsilon}{\partial x_1} + \frac{\varepsilon}{a}\frac{\partial P_\varepsilon}{\partial x_3} = 0, \tag{3.8}$$

$$-\varepsilon\Big(\frac{\partial^2 V_\varepsilon^2}{\partial x_2^2} + \frac{\partial^2 V_\varepsilon^2}{\partial x_3^2} - \frac{1}{a}\frac{\partial V_\varepsilon^2}{\partial x_2} - \frac{1}{a^2}V_\varepsilon^2\Big) + V_\varepsilon^2 + \frac{\partial P_\varepsilon}{\partial x_2} = 0, \tag{3.9}$$

$$-\varepsilon\Big(\frac{\partial^2 V_\varepsilon^3}{\partial x_2^2} + \frac{\partial^2 V_\varepsilon^3}{\partial x_3^2} - \frac{1}{a}\frac{\partial V_\varepsilon^3}{\partial x_2}\Big) + V_\varepsilon^3 + \frac{\partial P_\varepsilon}{\partial x_3} = Ra_D\theta_\varepsilon, \tag{3.10}$$

$$\frac{\partial V_\varepsilon^2}{\partial x_2}+\frac{\partial V_\varepsilon^3}{\partial x_3}-\frac{1}{a}V_\varepsilon^2-\frac{\varepsilon}{a}\frac{\partial V_\varepsilon^1}{\partial x_1}+\frac{\varepsilon}{a}\frac{\partial V_\varepsilon^1}{\partial x_3}=0, \tag{3.11}$$

$$\begin{aligned}&-\Big(\frac{\partial^2\theta_\varepsilon}{\partial x_2^2}+\frac{\partial^2\theta_\varepsilon}{\partial x_3^2}-\frac{1}{a}\frac{\partial\theta_\varepsilon}{\partial x_2}+\frac{x_2}{a^2}\frac{\partial\theta_\varepsilon}{\partial x_2}+\frac{\varepsilon^2}{a^2}\frac{\partial^2\theta_\varepsilon}{\partial x_1^2}-\frac{3x_2^2-\varepsilon^2}{a^2}\frac{\partial^2\theta_\varepsilon}{\partial x_3^2}\Big)\\&+\Big(\frac{\varepsilon}{a}\Big(1+\frac{x_2}{a}\Big)\Big(-\frac{\partial\theta_\varepsilon}{\partial x_1}+\frac{\partial\theta_\varepsilon}{\partial x_3}\Big)-\frac{\varepsilon x_3}{a^2}\frac{\partial\theta_\varepsilon}{\partial x_2}\Big)V_\varepsilon^1+\frac{\partial\theta_\varepsilon}{\partial x_2}V_\varepsilon^2\\&+\Big(\frac{\partial\theta_\varepsilon}{\partial x_3}+\frac{\varepsilon^2}{a^2}\frac{\partial\theta_\varepsilon}{\partial x_1}-\frac{x_2^2}{a^2}\frac{\partial\theta_\varepsilon}{\partial x_3}\Big)V_\varepsilon^3=0\qquad\text{in}\quad S_\varepsilon.\end{aligned} \tag{3.12}$$

Following [13], the Newton cooling condition $(2.12)_2$ on $(0,1)\times\varepsilon\partial B$ reads:

$$\begin{aligned}&\frac{1}{\varepsilon}\Big(x_2\frac{\partial\theta_\varepsilon}{\partial x_2}+x_3\frac{\partial\theta_\varepsilon}{\partial x_3}\Big)-\frac{1}{a\varepsilon}\Big(x_2^2\frac{\partial\theta_\varepsilon}{\partial x_2}+x_2x_3\frac{\partial\theta_\varepsilon}{\partial x_3}\Big)\\&\qquad-\frac{\varepsilon x_3}{a^2}\Big(\frac{\partial\theta_\varepsilon}{\partial x_1}-\frac{\partial\theta_\varepsilon}{\partial x_3}\Big)=Nu_\varepsilon(G-\theta_\varepsilon).\end{aligned} \tag{3.13}$$

4. Asymptotic expansion

In order to derive the asymptotic solution, we use the two-scale expansion with respect to ε and expand the unknowns from the system (3.8)–(3.12) as follows:

$$V_\varepsilon^1(x)=\varepsilon^2V_0^1\Big(x_1,\frac{x_2}{\varepsilon},\frac{x_3}{\varepsilon}\Big)+\varepsilon^3V_1^1\Big(x_1,\frac{x_2}{\varepsilon},\frac{x_3}{\varepsilon}\Big)+\dots, \tag{4.1}$$

$$V_\varepsilon^\alpha(x)=\varepsilon^3V_0^\alpha\Big(x_1,\frac{x_2}{\varepsilon},\frac{x_3}{\varepsilon}\Big)+\varepsilon^4V_1^\alpha\Big(x_1,\frac{x_2}{\varepsilon},\frac{x_3}{\varepsilon}\Big)+\dots\quad\alpha=2,3, \tag{4.2}$$

$$P_\varepsilon(x)=P_0\Big(x_1,\frac{x_2}{\varepsilon},\frac{x_3}{\varepsilon}\Big)+\varepsilon P_1\Big(x_1,\frac{x_2}{\varepsilon},\frac{x_3}{\varepsilon}\Big)+\varepsilon^2P_2\Big(x_1,\frac{x_2}{\varepsilon},\frac{x_3}{\varepsilon}\Big)+\dots, \tag{4.3}$$

$$\theta_\varepsilon(x)=\theta_0\Big(x_1,\frac{x_2}{\varepsilon},\frac{x_3}{\varepsilon}\Big)+\varepsilon\theta_1\Big(x_1,\frac{x_2}{\varepsilon},\frac{x_3}{\varepsilon}\Big)+\varepsilon^2\theta_2\Big(x_1,\frac{x_2}{\varepsilon},\frac{x_3}{\varepsilon}\Big)+\dots \tag{4.4}$$

The leading-order powers in the pressure and temperature expansion are clear an determined by the boundary conditions (2.13). However, to postulate the velocity expansion, one needs to take into account the specific scaling in the equations (3.8)–(3.11). Consequently, we obtain the ansatz which differs from the one for straight-pipe flow (see [22]). Now, we proceed in a standard manner: we substitute the expansions (4.1)–(4.4) into (3.8)–(3.12) and collect the terms with equal powers of ε.

4.1. Thermodynamic part. To begin with, we address the thermodynamic part of the system (3.12), (3.13). By comparing the Nusselt number Nu_{ep} with small parameter ε, we identify different effective behaviors of the heat flow, namely:

(1) $Nu^\varepsilon\gg\mathcal{O}(\varepsilon^3)$
By a simple calculation, one can easily verify that this assumption yields $\theta_0=G$ implying that the temperature of the surrounding medium dominates the process.

(2) $Nu^\varepsilon\ll\mathcal{O}(\varepsilon^3)$
Similarly, we deduce that, under this assumption, the effects of the heat

exchange through the lateral boundary would be negligible in the asymptotic model.

(3) $Nu^\varepsilon = \mathcal{O}(\varepsilon^3)$
This is, obviously, the critical (and the most interesting) case capturing all physically relevant effects that we seek for. In view of that, we are going to carry out our analysis for $Nu_\varepsilon = \varepsilon^3$. Naturally, Cases 1. and 2. can be treated in the same manner.

In the sequel, we employ the following notation:

$$\begin{aligned} \Delta_{y'}\Phi &= \frac{\partial^2\Phi}{\partial y_1^2} + \frac{\partial^2\Phi}{\partial y_2^2}, \\ \nabla_{y'}\Phi &= \frac{\partial\Phi}{\partial y_1}\mathbf{e}_2 + \frac{\partial\Phi}{\partial y_2}\mathbf{e}_3, \qquad y' = (y_2, y_3) = \Big(\frac{x_2}{\varepsilon}, \frac{x_3}{\varepsilon}\Big). \end{aligned} \tag{4.5}$$

The first term in the temperature expansion is given by the following Neumann problem:

$$\varepsilon^{-2} : \Delta_{y'}\theta_0 = 0 \text{ in } S = (0,1)\times B, \quad \varepsilon^{-1} : \nabla_{y'}\theta_0 \cdot y' = 0 \text{ on } \Gamma = (0,1)\times\partial B \tag{4.6}$$

implying $\theta_0 = \theta_0(x_1)$. The boundary-value problems satisfied by θ_i, $i = 1, 2$, are of the same form so we conclude $\theta_i = \theta_i(x_1)$, $i = 1, 2$. For the next term in the expansion we get

$$\varepsilon : \Delta_{y'}\theta_3 = 0 \text{ in } S, \quad \varepsilon^2 : \nabla_{y'}\theta_3 \cdot y' = \frac{y_3}{a^2}\frac{d\theta_0}{dx_1} \text{ on } \Gamma. \tag{4.7}$$

The problem (4.7) can be solved by taking

$$\theta_3(x_1, y_3) = \frac{1}{a^2}\frac{d\theta_0}{dx_1} y_3. \tag{4.8}$$

The problem describing θ_4 has the following form:

$$\begin{cases} \varepsilon^2 : \Delta_{y'}\theta_4 = -\frac{1}{a^2}\frac{d^2\theta_0}{dx_1^2} & \text{in } S, \\ \varepsilon^3 : \nabla_{y'}\theta_4 \cdot y' = \frac{y_2 y_3}{a}\frac{\partial\theta_3}{\partial y_3} + \frac{y_3}{a^2}\frac{d\theta_1}{dx_1} + (G - \theta_0) & \text{on } \Gamma. \end{cases} \tag{4.9}$$

The compatibility condition guaranteeing the solvability of (4.9) yields an ODE for θ_0:

$$\frac{1}{a^2}\frac{d^2\theta_0}{dx_1^2} + 2(G(x_1) - \theta_0) = 0 \text{ in } (0,1). \tag{4.10}$$

Taking into account the boundary conditions, namely $\theta_0(i) = T_i$, $i = 0, 1$, we obtain

$$\begin{aligned} \theta_0(x_1) = {} & T_0\cosh(\sqrt{2}ax_1) + A_1\sinh(\sqrt{2}ax_1) \\ & + \sqrt{2}a\bigg(\int_0^{x_1} G(\xi)\sinh(\sqrt{2}a\xi)d\xi\bigg)\cosh(\sqrt{2}ax_1) \\ & - \sqrt{2}a\bigg(\int_0^{x_1} G(\xi)\cosh(\sqrt{2}a\xi)d\xi\bigg)\sinh(\sqrt{2}ax_1), \end{aligned} \tag{4.11}$$

where the constant A_1 is given by

$$A_1 = \frac{T_1}{\sinh(\sqrt{2}a)} - T_0 \coth(\sqrt{2}a) - \sqrt{2}a\left(\int_0^1 G(\xi)\sinh(\sqrt{2}a\xi)d\xi\right)\coth(\sqrt{2}a) + \sqrt{2}a\left(\int_0^1 G(\xi)\cosh(\sqrt{2}a\xi)\right)d\xi. \tag{4.12}$$

Finally, it is straightforward to confirm that θ_4 is given by the following expression:

$$\theta_4(x_1, y') = -\frac{1}{4a^2}\frac{d^2\theta_0}{dx_1^2}|y'|^2 + \frac{1}{2a^3}\frac{d\theta_0}{dx_1}y_2y_3 + \frac{1}{a^2}\frac{d\theta_1}{dx_1}y_3. \tag{4.13}$$

4.2. Hydrodynamic part. Now we turn our attention to the hydrodynamic part of the system (3.8)–(3.11). The lowest-order term gives $\frac{\partial P_0}{\partial y_\alpha} = 0$ $(\alpha = 2, 3)$ implying $P_0 = P_0(x_1)$. Moreover, from (3.9)–(3.10), we deduce $\frac{\partial P_1}{\partial y_2} = 0$ and $\frac{\partial P_1}{\partial y_3} = Ra_D\theta_0(x_1)$ leading to

$$P_1(x_1, y_3) = Ra_D\theta_0(x_1)y_3 + P_1^0(x_1). \tag{4.14}$$

The next term is given by $\frac{\partial P_2}{\partial y_2} = 0$ and $\frac{\partial P_2}{\partial y_3} = Ra_D\theta_1(x_1)$ so we have

$$P_2(x_1, y_3) = Ra_D\theta_1(x_1)y_3 + P_2^0(x_1). \tag{4.15}$$

We proceed by identifying the problem for the velocity zero-order approximation:

$$\varepsilon : -\Delta_{y'}V_0^1 - \frac{1}{a}\frac{dP_0}{dx_1} + \frac{1}{a}\frac{dP_1}{dy_3} = -\Delta_{y'}V_0^1 - \frac{1}{a}\frac{dP_0}{dx_1} + \frac{1}{a}Ra_D\theta_0(x_1) = 0, \tag{4.16}$$

$$\varepsilon^2 : -\Delta_{y'}V_0^2 + \frac{\partial P_3}{\partial y_2} = 0, \quad -\Delta_{y'}V_0^3 + \frac{\partial P_3}{\partial y_3} = Ra_D\theta_2(x_1), \tag{4.17}$$

$$\varepsilon^2 : \operatorname{div}_{y'} V_0 = \frac{\partial V_0^2}{\partial y_2} + \frac{\partial V_0^3}{\partial y_3} = -\frac{1}{a}\frac{\partial V_0^1}{\partial y_3} \text{ in } S. \tag{4.18}$$

In view of the no-slip boundary condition for the velocity, we deduce $V_0^2 = 0$, $P_3 = P_3(x_1, y_3)$ and

$$V_0^1 = \frac{1}{4a}(1 - |y'|^2)\Big(- Ra_D\theta_0(x_1) + \frac{dP_0}{dx_1}\Big), \tag{4.19}$$

$$V_0^2 = 0, \quad P_3 = P_3(x_1, y_3), \tag{4.20}$$

$$V_0^3 = -\frac{1}{a}V_0^1. \tag{4.21}$$

From $(4.17)_2$ and (4.21) it follows

$$\frac{1}{a}\Delta_{y'}V_0^1 + \frac{\partial P_3}{\partial y_3} = Ra_D\theta_2(x_1) \tag{4.22}$$

implying

$$P_3(x_1, y_3) = \Big(Ra_D\theta_2(x_1) - \frac{1}{a^2}Ra_D\theta_0(x_1) + \frac{1}{a^2}\frac{dP_0}{dx_1}\Big)y_3 + P_3^0(x_1), \tag{4.23}$$

due to (4.19).

Note that we still have to compute the pressure $P_0(x_1)$ and, of course, the velocity corrector.

4.3. Velocity corrector. The first component of the velocity corrector is to be determined from the momentum equation (3.8):

$$\varepsilon^2 : -\Big(\Delta_{y'} V_1^1 + \frac{1}{a}\frac{\partial V_0^1}{\partial y_2}\Big) + V_0^1 - \frac{1}{a}\frac{\partial P_1}{\partial x_1} + \frac{1}{a}\frac{\partial P_2}{\partial y_3} = 0 \text{ in } S. \tag{4.24}$$

Taking into account the obtained expressions for V_0^1, P_1 and P_2 from Sec. 4.2, we arrive at

$$\begin{aligned}\Delta_{y'} V_1^1 = {}& \frac{1}{2a^2}\Big(- Ra_D\theta_0(x_1) + \frac{dP_0}{dx_1}\Big) y_2 \\ & + \frac{1}{4a}(1 - |y'|^2)\Big(- Ra_D\theta_0(x_1) + \frac{dP_0}{dx_1}\Big) \\ & - \frac{1}{a} Ra_D \frac{d\theta_0}{dx_1} y_3 + \frac{1}{a} Ra_D \theta_1(x_1).\end{aligned} \tag{4.25}$$

The remaining two components of the velocity corrector are then deduced from the divergence equation (3.11):

$$\varepsilon^3 : \operatorname{div}_{y'} V_1 = \frac{1}{a}\frac{\partial V_0^1}{\partial x_1} - \frac{1}{a}\frac{\partial V_1^1}{\partial y_3}. \tag{4.26}$$

However, observe that first we have to compute the corrector θ_1 appearing in (4.25). To accomplish that, we go back to the heat equation (3.12) and identify the problem for θ_5:

$$\begin{aligned}&\varepsilon^3 : -\Big(\Delta_{y'}\theta_5 - \frac{1}{a}\frac{\partial\theta_4}{\partial y_2} + \frac{1}{a^2}\frac{d^2\theta_1}{dx_1^2}\Big) - \frac{1}{a}\frac{d\theta_0}{dx_1} V_0^1 = 0 \text{ in } S, \\ &\varepsilon^4 : \nabla_{y'}\theta_5 \cdot y' = \frac{1}{a} y_2^2 \frac{\partial\theta_4}{\partial y_2} + \frac{1}{a} y_2 y_3 \frac{\partial\theta_4}{\partial y_3} + \frac{y_3}{a^2}\frac{d\theta_2}{dx_1} - \frac{y_3}{a^2}\frac{\partial\theta_3}{\partial y_3} - \theta_1 \text{ on } \Gamma.\end{aligned} \tag{4.27}$$

Applying the expressions (4.8) and (4.13) for θ_3 and θ_4, we get

$$\begin{aligned}\Delta_{y'}\theta_5 = {}& -\frac{1}{a^2}\frac{d^2\theta_1}{dx_1^2} - \frac{1}{2a^3}\frac{d^2\theta_0}{dx_1^2} y_2 + \frac{1}{2a^4}\frac{d\theta_0}{dx_1} y_3 - \frac{1}{a}\frac{d\theta_0}{dx_1} V_0^1 \text{ in } S, \\ \nabla_{y'}\theta_5 \cdot y' = {}& -\frac{1}{2a^3}\frac{d^2\theta_0}{dx_1^2} y_2 + \frac{1}{a^4}\frac{d\theta_0}{dx_1} y_2^2 y_3 \\ & + \frac{1}{a^3} y_2 y_3 \frac{d\theta_1}{dx_1} + \Big(\frac{1}{a^2}\frac{d\theta_2}{dx_1} - \frac{1}{a^4}\frac{d\theta_0}{dx_1}\Big) y_3 - \theta_1 \text{ on } \Gamma.\end{aligned} \tag{4.28}$$

In view of (4.19), the compatibility condition related to (4.28) yields an ODE for θ_1:

$$\frac{d^2\theta_1}{dx_1^2} - 2a^2\theta_1 = -\frac{1}{8}\frac{d\theta_0}{dx_1}\Big(- Ra_D\theta_0(x_1) + \frac{dP_0}{dx_1}\Big) \text{ in } (0,1). \tag{4.29}$$

Endowing it with the boundary conditions $\theta_1(0) = \theta_1(1) = 0$, we obtain

$$\theta_1(x_1) = A_2 \sinh(\sqrt{2}ax_1) + \sqrt{2}a\Big(\int_0^{x_1} H(\xi)\sinh(\sqrt{2}a)d\xi\Big)\cosh(\sqrt{2}ax_1) \tag{4.30}$$

$$- \sqrt{2}a\Big(\int_0^{x_1} H(\xi)\cosh(\sqrt{2}a)d\xi \Big) \sinh(\sqrt{2}ax_1),$$

with

$$H(x_1) = \frac{1}{16a^2}\frac{d\theta_0}{dx_1}\Big(- Ra_D\theta_0(x_1) + \frac{dP_0}{dx_1}\Big),$$

$$\begin{aligned} A_2 = &-\sqrt{2}a\Big(\int_0^{1} H(\xi)\sinh(\sqrt{2}a)d\xi \Big) \coth(\sqrt{2}a) \\ &+ \sqrt{2}a\Big(\int_0^{1} H(\xi)\cosh(\sqrt{2}a)d\xi \Big) \sinh(\sqrt{2}a). \end{aligned} \tag{4.31}$$

We can also explicitly calculate $\theta_5(x_1, y')$ from (4.28) as:

$$\begin{aligned} \theta_5(x_1,y') = &- \frac{1}{4a^2}\frac{d^2\theta_1}{dx_1^2}|y'|^2 - \frac{y_2}{16a^3}\frac{d^2\theta_0}{dx_1^2}(|y'|^2+5) \\ &+ \frac{y_3}{16a^4}\frac{d\theta_0}{dx_1}\Big(5|y'|^2 - \frac{16}{3}y_3^2 + 1\Big) \\ &+ \frac{1}{2a^3}\frac{d\theta_1}{dx_1}y_2y_3 + \Big(\frac{1}{a^2}\frac{d\theta_2}{dx_1} - \frac{1}{a^4}\frac{d\theta_0}{dx_1}\Big)y_3 \\ &- \frac{1}{a^2}\frac{d\theta_0}{dx_1}\Big(\frac{|y'|^2}{16} - \frac{|y'|^4}{64}\Big)\Big(- Ra_D\theta_0 + \frac{dP_0}{dx_1}\Big). \end{aligned} \tag{4.32}$$

Now, we are in position to compute V_1^1 from (4.25) and $V_1^1 = 0$ on Γ. As a result, we obtain

$$\begin{aligned} V_1^1(x_1,y') = &\frac{1}{16a^2}\Big(Ra_D\theta_0(x_1) - \frac{dP_0}{dx_1}\Big)y_2(1-|y'|^2) \\ &+ \frac{1}{a}\Big(- Ra_D\theta_0(x_1) + \frac{dP_0}{dx_1}\Big)\Big(\frac{|y'|^2}{16} - \frac{|y'|^4}{64} - \frac{3}{64}\Big) \\ &+ \frac{1}{8a}Ra_D\frac{d\theta_0}{dx_1}y_3(1-|y'|^2) - \frac{1}{4a}Ra_D\theta_1(x_1)(1-|y'|^2). \end{aligned} \tag{4.33}$$

To determine $P_0(x_1)$, we integrate (4.26) over B. We have

$$\begin{aligned} &\int_B \Big[\frac{1}{4a}(1-|y'|^2)\Big(- Ra_D\frac{d\theta_0}{dx_1} + \frac{d^2P_0}{dx_1^2}\Big)\Big]dy' \\ &= \int_B \Big[\frac{1}{8a^2}\Big(- Ra_D\theta_0(x_1) + \frac{dP_0}{dx_1}\Big)y_2y_3 \\ &\qquad + \frac{1}{a}\Big(- Ra_D\theta_0(x_1) + \frac{dP_0}{dx_1}\Big)\Big(\frac{y_3}{8} - \frac{y_2^2y_3 + y_3^3}{16}\Big) \\ &\qquad + \frac{1}{8a}Ra_D\frac{d\theta_0}{dx_1}(1-y_2^2-3y_3^2) + \frac{1}{2a}Ra_D\theta_1(x_1)y_3\Big]dy'. \end{aligned} \tag{4.34}$$

By passing to polar coordinates, one can easily check that all the integrals on the right-hand side in (4.34) vanish. Hence

$$\frac{\pi}{8a}\Big(- Ra_D\frac{d\theta_0}{dx_1} + \frac{d^2P_0}{dx_1^2}\Big) = 0 \tag{4.35}$$

providing

$$P_0(x_1) = Ra_D \int_0^{x_1} \theta_0(\xi)d\xi + A_3\, x_1 + A_4. \tag{4.36}$$

The constants A_3, A_4 are determined by employing the boundary conditions $P_0(i) = q_i$, $i = 0, 1$, namely

$$A_3 = q_1 - q_0 - Ra_D \int_0^1 \theta_0(\xi)d\xi, \quad A_4 = q_0. \tag{4.37}$$

It is important to notice that

$$-Ra_D\theta_0(x_1) + \frac{dP_0}{dx_1} = A_3 = \text{const.} \tag{4.38}$$

so from (4.19) we deduce that $V_0^1 = V_0^1(y')$. As a consequence, from (4.26), we get

$$\operatorname{div}_{y'} V_1 = \frac{\partial V_1^2}{\partial y_2} + \frac{\partial V_1^3}{\partial y_3} = -\frac{1}{a}\frac{\partial V_1^1}{\partial y_3} \tag{4.39}$$

which can be solved by taking

$$V_1^2 = 0, \quad V_1^3 = -\frac{1}{a}V_1^1. \tag{4.40}$$

This completes the derivation of the velocity corrector. It only remains to compute $\theta_2(x_1)$. For that purpose, we have to look at the problem for θ_6:

$$\begin{aligned}
&\varepsilon^4 : -\Big(\Delta_{y'}\theta_6 - \frac{1}{a}\frac{\partial\theta_5}{\partial y_2} + \frac{y_2}{a^2}\frac{\partial\theta_4}{\partial y_2} + \frac{1}{a^2}\frac{\partial^2\theta_2}{\partial x_1^2} - \frac{3y_2^2-1}{a^2}\frac{\partial^2\theta_4}{\partial y_3^2}\Big)\\
&\qquad - \frac{1}{a}\frac{\partial\theta_0}{\partial x_1}V_1^1 - \frac{y_2}{a^2}\frac{d\theta_0}{dx_1}V_0^1 - \frac{1}{a}\frac{d\theta_1}{dx_1}V_0^1 = 0 \text{ in } S,\\
&\varepsilon^5 : \nabla_{y'}\theta_6 \cdot y' = \frac{1}{a}y_2^2\frac{\partial\theta_5}{\partial y_2} + \frac{1}{a}y_2y_3\frac{\partial\theta_5}{\partial y_3} + \frac{y_3}{a^2}\frac{\partial\theta_3}{\partial x_1} - \frac{y_3}{a^2}\frac{\partial\theta_4}{\partial y_3} - \theta_2 \text{ on } \Gamma.
\end{aligned} \tag{4.41}$$

In view of the previous results, it is straightforward to confirm that the compatibility condition ensuring the solvability of the problem (4.41) gives

$$\frac{d^2\theta_2}{dx_1^2} - 2a^2\theta_2 = -2a^2 J(x_1), \tag{4.42}$$

with

$$\begin{aligned}
J(x_1) = {}& \frac{3}{16a^4}\frac{d^2\theta_0}{dx_1^2} - \frac{1}{16a^4}\frac{d^2\theta_0}{dx_1^2} - \frac{1}{16a^4}\frac{d^2\theta_0}{dx_1^2}\\
&- \frac{3}{256a^2}\frac{d\theta_0}{dx_1}\Big(Ra_D\theta_0(x_1) - \frac{dP_0}{dx_1}\Big) - \frac{d\theta_0}{dx_1}\frac{1}{16a^2}Ra_D\theta_1(x_1)\\
&- \frac{1}{32a^2}\frac{d\theta_1}{dx_1}\Big(Ra_D\theta_0 - \frac{dP_0}{dx_1}\Big) - \frac{89}{96a^4}\frac{d^2\theta_0}{dx_1^2}\\
&- \frac{1}{256a^4}\frac{d^2\theta_0}{dx_1^2} + \frac{1}{4a^4}\frac{d^2\theta_0}{dx_1^2} + \frac{1}{8a^4}\frac{d^2\theta_0}{dx_1^2}.
\end{aligned} \tag{4.43}$$

Due to the boundary conditions $\theta_2(0) = \theta_2(1) = 0$, we finally obtain

$$\theta_2(x_1) = A_5 \sinh(\sqrt{2}ax_1) + \sqrt{2}a\left(\int_0^{x_1} J(\xi)\sinh(\sqrt{2}a\xi)d\xi \right) \cosh(\sqrt{2}ax_1) - \sqrt{2}a\left(\int_0^{x_1} J(\xi)\cosh(\sqrt{2}a\xi)d\xi \right) \sinh(\sqrt{2}ax_1), \tag{4.44}$$

where the constant A_5 is given by

$$A_5 = -\sqrt{2}a\left(\int_0^{1} J(\xi)\sinh(\sqrt{2}a\xi)d\xi \right) \coth(\sqrt{2}a) + \sqrt{2}a\left(\int_0^{1} J(\xi)\cosh(\sqrt{2}a\xi)d\xi \right) \sinh(\sqrt{2}a). \tag{4.45}$$

5. Results and discussion

To summarize, let us write the obtained asymptotic solution. The approximations for the filtration velocity and the pressure have the form:

$$\mathbf{u}_\varepsilon^{\text{approx}}(z) = \mathbf{V}_\varepsilon(x), \quad z = \mathbf{\Phi}_\varepsilon(x), \quad \mathbf{V}_\varepsilon = \mathcal{V}_\varepsilon^1 \mathbf{e}_\varepsilon + \mathcal{V}_\varepsilon^3 \mathbf{e}_1, \tag{5.1}$$

$$\mathcal{V}_\varepsilon^1(x) = \varepsilon^2 V_0^1\left(\frac{x'}{\varepsilon}\right) + \varepsilon^3 V_1^1\left(x_1, \frac{x'}{\varepsilon}\right), \tag{5.2}$$

$$\mathcal{V}_\varepsilon^3(x) = \varepsilon^3 V_0^3\left(\frac{x'}{\varepsilon}\right) + \varepsilon^4 V_1^3\left(x_1, \frac{x'}{\varepsilon}\right), \tag{5.3}$$

$$p_\varepsilon^{\text{approx}}(z) = \Pi_\varepsilon(x), \quad z = \mathbf{\Phi}_\varepsilon(x), \tag{5.4}$$

$$\Pi_\varepsilon(x) = P_0(x_1) + \varepsilon P_1\left(x_1, \frac{x_3}{\varepsilon}\right) + \varepsilon^2 P_2\left(x_1, \frac{x_3}{\varepsilon}\right) + \varepsilon^3 P_3\left(x_1, \frac{x_3}{\varepsilon}\right). \tag{5.5}$$

It should be emphasized that all the components in the above solution have been computed in the explicit form, see Section 4. Using (4.19)–(4.21), it is straightforward to confirm that the zero-order approximation, namely $\mathbf{V}_\varepsilon^0 = \varepsilon^2 V_0^1 \mathbf{e}_\varepsilon + \varepsilon^3 V_0^3 \mathbf{e}_1$, is as the one obtained for the straight-pipe flow in [22], of course, in the direction tangential to the central curve of the pipe. Here we do not detect the effects of the specific pipe's geometry. For that reason, we correct the zero-order approximation by computing the lower-order term in the asymptotic expansion. The effects of pipe's distortion are captured by the first-order corrector, whose components are given by (4.33) and (4.40). The first part of asymptotic approximation for the pressure does not exhibit the effects of the pipe's curvedness (see (4.14), (4.15), (4.36)), whereas the third-order corrector feels those effects (see (4.23)).

The approximation for the fluid temperature reads:

$$T_\varepsilon^{\text{approx}}(z) = \Theta_\varepsilon(x), \quad z = \mathbf{\Phi}_\varepsilon(x), \tag{5.6}$$

$$\Theta_\varepsilon(x) = \theta_0(x_1) + \varepsilon\theta_1(x_1) + \varepsilon^2\theta_2(x_1) + \varepsilon^3\theta_3\left(x_1, \frac{x_3}{\varepsilon}\right) + \varepsilon^4\theta_4\left(x_1, \frac{x'}{\varepsilon}\right) + \varepsilon^5\theta_5\left(x_1, \frac{x'}{\varepsilon}\right). \tag{5.7}$$

The functions θ_i are given by the explicit formulae (4.8), (4.11), (4.13), (4.30), (4.32) and (4.44). Comparing with the result from [22], we observe that the first-order approximation $\theta_0 + \varepsilon\theta_1$ is consistent with the one obtained for the straight-pipe flow. The effects of the pipe's distortion are clearly detected in θ_2 and in all forthcoming terms.

The higher-order asymptotic model described by (5.1)–(5.7) provides an excellent platform for understanding the direct influence of the pipe's helical geometry on the effective flow and heat transfer through a porous medium. The asymptotic solution, as provided here in the explicit form, can be used as a check on computer models for real helical-pipe flows. From the strictly mathematical point of view, formally derived model should be rigorously justified by proving the corresponding error estimate. To accomplish that, the natural way would be to use the same arguments as we did in a straight-pipe case (see [22]). However, due to the complexity of the flow domain (and, thus, the flow equations), additional terms appear preventing us to construct the divergence correction in a standard manner. As a result, we are not in position to derive satisfactory error estimates acknowledging the correctors. Nevertheless, we believe that this technical difficulty can be overcome and this is the subject of our current investigation.

Acknowledgments. This research has been supported by the *Croatian Science Foundation* (scientific project 3955: *Mathematical modeling and numerical simulations of processes in thin or porous domains*).

References

1. W. R. Dean, *Note on the motion of fluid in a curved pipe*, Phil. Mag. (7) **4** (1927), 208–223.
2. C. Y. Wang, *On the low-Reynolds-number flow in a helical pipe*, J. Fluid Mech. **108** (1981), 185–194.
3. M. Germano, *On the effect of torsion on a helical pipe flow*, J. Fluid Mech. **125** (1982), 1–8.
4. M. Germano, *The Dean equations extended to a helical pipe flow*, J. Fluid Mech. **203** (1989), 289–305.
5. K. Yamamoto, T. Akita, H. Ikeuchi, Y. Kita, *Experimental study of the flow in a helical circular tube*, Fluid Dyn. Res. **16** (1995), 237–249.
6. T. J. Hüttl, R. Friedrich, *Direct numerical simulation of turbulent flows in curved and helically coiled pipes*, Comput. Fluids **30** (2001), 591–605.
7. J-W. Wang, J. R. G. Andrews, *Numerical simulation of flow in helical ducts*, AIChE J. **41**(5) (2004), 1071–1080.
8. K. Yamamoto, A. Aribowo, Y. Hayamizu, T. Hirose, K. Kawahara, *Visualization of the flow in a helical pipe*, Fluid Dyn. Res. **30** (2002), 251
9. E. Marušić-Paloka, I. Pažanin, *Effective flow of a viscous liquid through a helical pipe*, C. R., Méc., Acad. Sci. Paris **332** (2004), 973–978.
10. E. Marušić-Paloka E., I. Pažanin, *Fluid flow through a helical pipe*, Z. Angew. Math. Phys. **58** (2007), 81–99.
11. I. Pažanin, *Investigation of micropolar fluid flow in a helical pipe via asymptotic analysis*, Commun. Nonlinear Sci. Numer. Simul. **18** (2013) 528–540.
12. P. Naphon, S. Wongwises, *A review of flow and heat transfer characteristics in curved tubes*, Renewable & Sustainable Energy Reviews **10**(5) (2006), 463–490.
13. E. Marušić-Paloka, I. Pažanin, *Modelling of heat transfer in a laminar flow thorugh a helical pipe*, Math. Comput. Modelling **50** (2009), 1571–1582.
14. E. Marušić-Paloka, I. Pažanin, *On the effects of curved geometry on heat conduction through a distorted pipe*, Nonlinear Anal., Real World Appl. **11** (2010), 4554–4564.

15. E. Marušić-Paloka, I. Pažanin, S. Marušić, *Comparison between Darcy and Brinkman laws in a fracture*, Appl. Math. Comput. **218**(14) (2012), 7538–7545.
16. I. Pažanin, P. G. Siddheshwar, *Analysis of the laminar Newtonian fluid flow through a thin fracture modelled as fluid-saturated sparsely packed porous medium*, Z. Nat.forsch., A: Phys. Sci. **72**(3) (2017) 253–259.
17. D. A. Nield, A. Bejan, *Convection in Porous Media*, Springer-Verlag, New York (2006).
18. J. P. Kelliher, R. Temam, X. Wang, *Boundary layer associated with the Darcy–Brinkman–Boussinesq model for convection porous media*, Physica D **240** (2011) 619–628.
19. S. Srinivasan, K. R. Rajagopal, *A thermodynamic basis for the derivation of the Darcy, Forchheimer and Brinkman models for flows through porous media and their generalizations*, Int. J. Non-Linear Mech. **58** (2014), 162–166.
20. K. Hooman, A. A. Ranjbar-Kani, *A perturbation based analysis to investigate forced convection in a porous saturated tube*, J. Comput. Appl. Math. **162**(2) (2004), 411–419.
21. M. T. Jamal-Abad, S. Saedodin, M. Aminy, *Variable conductivity in forced convection for a tube filled with porous media: A perturbation solution*, Ain Shams Engineering Journal (2016), http://dx.doi.org/10.1016/j.asej.2016.03.019.
22. M. Beneš, I. Pažanin, *Rigorous derivation of the effective model describing a non-isothermal fluid flow in a vertical pipe filled with porous medium*, Continuum Mech. Thermodyn. **30** (2018), 301–317.
23. D. Nield, A. V. Kuznetsov, *Forced convection in a helical pipe filled with a saturated porous medium*, Int. J. Heat Mass Transfer **47**(24) (2004), 5175–5180.
24. L. Cheng, A. V. Kuznetsov, *Heat transfer in a laminar flow in a helical pipe filled with a fluid saturated porous medium*, International Journal of Thermal Sciences **44**(8) (2005), 787–798.

АСИМПТОТСКО РЕШЕЊЕ DARCY–BRINKMAN–BOUSSINESQ–ОВ ТОКА У ЦЕВИ ХЕЛИКОИДНОГ ОБЛИКА

Резиме. Проучавамо проток флуида и пренос топлоте у хеликоидним цевима испуњеном порозном средином. Мотивисана применама у инжењству, дебљина цеви и растојање између две завојнице спирале имају исти мали ред величине, са претпоставком да се флуид унутар цеви хлади (или загрева) под утицајем спољне средине. У бездимензионом Darcy–Brinkman–Boussinesq-ом систему написаним у криволинијским координатама, користили смо технику вишенивовског проширења ради формалног извођења ефективног модела применљивог за мали Brinkman–Darcy-јев број. Добијено асимптотско решење је дато у експлицитној форми која је важна за нумеричке симулације. Такође је дато поређење са нашим претходним резултатима везаним за протоке кроз праве цеви.

Department of Mathematics
Faculty of Science
University of Zagreb
Zagreb
Croatia
pazanin@math.hr

(Received 24.04.2018)
(Available online 05.07.2018)